ELSEVIER

journal homepage: www.elsevier.com/locate/jmatprotec

Influence of particle temperature and velocity on the microstructure and mechanical behaviour of high velocity oxy-fuel (HVOF)-sprayed nanostructured titania coatings

M. Gaona[a], *R.S. Lima*[b,*], *B.R. Marple*[b]

[a] *Thermal Spray Centre, Universitat de Barcelona, Martí i Franquès 1, 08028 Barcelona, Spain*
[b] *National Research Council of Canada, 75 de Mortagne Blvd., Boucherville, Que. J4B 6Y4, Canada*

ARTICLE INFO

Article history:
Received 8 May 2007
Received in revised form
17 July 2007
Accepted 17 July 2007

Keywords:
Thermal spray
High velocity oxy-fuel (HVOF)
In-flight particle diagnostics
Nanostructured titania (TiO_2)
Microstructure
Bond strength

ABSTRACT

Nanostructured titania feedstock powders were deposited via high velocity oxy-fuel (HVOF) spraying onto Ti–6Al–4V substrates. Using in-flight particle diagnostics, different particle temperatures and velocities were employed in order to reveal their effects on microstructure and mechanical properties of the coatings. A series of linear dependencies were observed involving processing conditions (i.e., in-flight particle temperature and velocity) and characteristics of the resulting coating microstructural features and properties, such as, phase composition, Vickers microhardness and the deflection of Almen strips (residual stress). High-bond strength values were observed when compared with other ceramic thermal spray coatings available in the literature. This study provides different levels of information on the processing of nanostructured ceramic powders via HVOF spraying and opens possibilities for development and application of HVOF-sprayed nanostructured titania coatings in the biomedical field and other disciplines, where superior mechanical behaviour is required.

1. Introduction

1.1. *Nanostructured materials*

Nanotechnology is an expanding field of research where studies of a fundamental nature are providing opportunities for successful application in a number of fields. Intense research efforts are underway to use nanotechnology to enhance properties and produce new materials in the medical, structural, electronic and magnetic fields. The so-called conventional materials exhibit grain sizes ranging from microns to millimetres, whereas, nanocrystalline materials are characterized by grain sizes below 100 nm. Different studies reveal that by decreasing the grain size to the nanostructured level there can be an important increase in grain boundaries that influences the chemical and physical properties of the material, which can differ substantially from those of conventional materials (Tjong and Chen, 2004). For example, nanoceramic materials can exhibit improved mechanical properties and even superplas-

* Corresponding author. Tel.: +1 450 641 5150; fax: +1 450 641 5105.
E-mail address: rogerio.lima@cnrc-nrc.gc.ca (R.S. Lima).
0924-0136/$ – see front matter © 2007 Elsevier B.V. All rights reserved.
doi:10.1016/j.jmatprotec.2007.07.024

ticity when compared to coarser-grained ceramics (Wakai et al., 1999).

1.2. *Biomedical applications of nanomaterials*

Because of the potential advantages of reducing the scale of the internal structure, there is a considerable effort focused on the use of nanostructured materials in the biomedical field. It is widely accepted that the interaction between cells and biocompatible surfaces is essential to a wide range of disciplines, such as, tissue engineering, biotechnologies, implant materials and cell-based sensors (Castner and Ratner, 2002; Kasemo, 2002). Different studies are focused on the possible use of nanostructured materials in prosthetic devices, since it is believed they can be designed to have surfaces and mechanical properties similar to those of physiological bone. It has been reported that materials exhibiting nanotextures on their surfaces will have an advantage in the interaction between the implant with the bone cells (e.g., osteoblasts) (Gutwein and Webster, 2004; Webster et al., 2000). It is hypothesized that the use of nanostructured coatings containing regions on the surface exhibiting nanotexture (nanoroughness) could be an interesting method to improve the adhesion of the osteoblast cells on the coating surface, leading to a better long-term performance of the implant. It is believed that the nanotopography enhances the adsorption of extracellular matrix (ECM) adhesion proteins such as collagen, fibronectin, thrombospondin, vitronectin, and osteopontin, for cell integrin receptors (Petit and Thiery, 2000). These adhesion proteins are initially adsorbed on the prosthesis surface almost immediately upon its implantation in the human body. Cellular interactions with ECM molecules are supposed to produce specific signals that are transduced through the integrins to the cytoplasm, the cytoskeleton, and the nucleus of the osteoblasts (Degasne et al., 1999). Compared with conventional alumina and titania, osteoblast adhesion increased by 46% and 30% on nanophase 23-nm grain size alumina and on nanophase 32-nm grain size titania, respectively (Webster et al., 1999).

1.3. *Applications of nanostructured titania thermally sprayed coatings*

Nanostructured titania thermally sprayed coatings have demonstrated excellent structural performance for anti-wear applications when compared to conventional titania coatings (Kim, 2004), mainly when the nanostructured feedstock powder is processed via high velocity oxy-fuel (HVOF) (Lima and Marple, 2006). This type of anti-wear coating has been used with success in high-pressure acid leach hydrometallurgical processing equipment, which employs autoclaves, valves and piping in a severe high-temperature acidic slurry environment (Kim, 2006).

Recently, the use of nanostructured titania thermally sprayed coatings in the biomedical field has also been investigated (Liu et al., 2005; Zhao et al., 2006; Legoux et al., 2006). The impetus for this recent work centres around the ongoing discussion about the stability of thermally sprayed hydroxyapatite (HA) coatings once implanted in vivo. Although the biocompatible and osteoconductive properties of HA coatings are well accepted (Bauer et al., 1991), an important drawback comes from the instability of the substrate/coating interface and the potential for accelerated deterioration of the coating in the presence of body fluids under local loading. For that reason the employment of a stable biocompatible and nanostructured coating material, such as titania, could be a promising alternative to HA coatings on prosthetic devices.

Considering that, the aim of the present work was to further investigate the HVOF processing of nanostructured titania powders to produce coatings that combine enhanced mechanical performance with nanotexturization of their surfaces, envisioning biomedical applications.

2. Experimental procedure

2.1. *Feedstock powder, thermal spraying and residual stress*

Nanostructured-titania (TiO_2) feedstock powder (VHP-DCS (5–20 μm)), Altair Nanomaterials Inc., Reno, NV, USA) was employed in this work. The particle size was measured by a laser diffraction particle size analyzer (Beckman Coulter LS 13320, Beckman Coulter, Miami, FL, USA) and the morphology was studied by means a field emission scanning electron microscopy (FE-SEM) (S-4700, Hitachi, Tokyo, Japan). The feedstock powder was agglomerated and sintered and exhibited a nominal particle distribution from 5 μm to 20 μm, according to the powder manufacturer.

The powder was thermally sprayed onto previously grit-blasted Ti–6Al–4V substrates by using an oxygen–propylene HVOF torch (Diamond Jet 2700-hybrid, Sulzer Metco, Westbury, NY, USA). Particle diagnostics (temperature and velocity) was carried out based on an in-flight diagnostic tool (DPV 2000, Tecnar Automation, Saint Bruno, QC, Canada). This diagnostic system is based on optical pyrometry and time-of-flight measurements that allows on-line measurements of the distributions of particle temperature, velocity and diameter in the spray jet. A total of 5000 particles were measured at the centreline of the spray jet, where the particle flow was the highest,

Table 1 – HVOF spray parameters and average particle temperature and velocity for each set of spray conditions (oxygen flow: 279 lpm; air flow: 202 lpm)

Propylene flow (lpm)	Spray distance (cm)	T (°C) (n = 5000)	V (m/s) (n = 5000)
65	20	1840 ± 150	647 ± 86
70	20	1881 ± 162	686 ± 93
90	18	2073 ± 141	854 ± 112

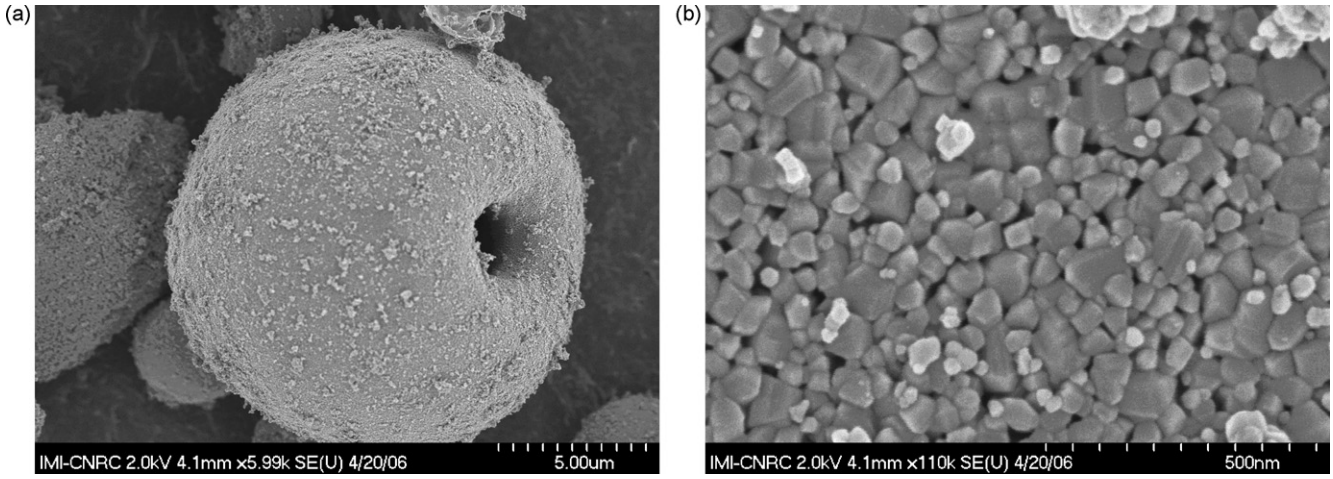

Fig. 1 – (a) Typical morphology of agglomerated spray-dried titania powders. (b) High magnification view of (a)—agglomeration of individual nanosized titania particles.

for each of the three spray conditions employed in this work. The particle detector was placed at the same spray distance as used when depositing the coatings (Table 1).

Considering the spray parameters, it was decided from previous experience to maintain the oxygen and air flows of the HVOF torch constant at 279 and 202 l per minute (lpm) and vary the propylene flow. After a series of tests that involved variations of propylene flow, three sets of spray parameters were chosen (see Table 1): two sets that exhibited average particle temperature levels approximately 20 °C above and below the melting point of titania (1855 °C) (Miyayama et al., 1991), and a third set that exhibited the highest particle temperature and velocity that could be produced without causing damage to the spray torch from the excessive heat of the flame. The powder feed rate and the carrier gas (N_2) flow were kept constant at 10 g/min and 54 lpm, respectively. A statistical software (StatGraphics Plus 2.0, Statistical Graphics, Rockville, MD, USA) was employed to determine the correlations among the spray parameters, in-flight particle characteristics and microstructural features.

During the spraying process a cooling system (air jets) was applied to reduce the coating temperature, which was monitored using a pyrometer. The maximum surface temperatures for the coatings were approximately 130 °C, 160 °C and 250 °C for the propylene flows of 65 lpm, 70 lpm and 90 lpm, respectively (Table 1).

Coatings were evaluated for residual stress by Almen strips (type N; grade I) (Electronics Inc., Mishawaka, IN, USA) that were mounted alongside the substrates and coated during the spraying process. The arc height (deflection) on the Almen strip was measured after grit blasting the surface (first reading) and again after coating application (second reading). The deflections of the Almen strips were read via an Almen gauge (Model TSP-3, Electronics Inc., Mishawaka, IN, USA), and reported as the difference of the two readings, second reading minus the first reading. Positive or negative deflection values were considered to represent tensile or compressive residual stress levels, respectfully. The absence of Almen deflection was considered as non-significant or neutral stress level. More details about the Almen strip technique for the evaluation of residual stress levels can be found elsewhere (Sauer and Sahoo, 2001).

2.2. *Microstructure, porosity and phase characterization*

The powder morphology and cross-sections of the coatings were examined by means of an FE-SEM to observe the microstructures from low magnifications up to a nanostructural level. For the observation of the cross-section and determination of the coating porosity, the samples were cut, vacuum impregnated with a low-viscosity epoxy resin and polished up to alumina emulsion. Digital image analysis was used to determine the porosity on these cross-sections. A total of 10 images per coating were analyzed to determine the porosity levels.

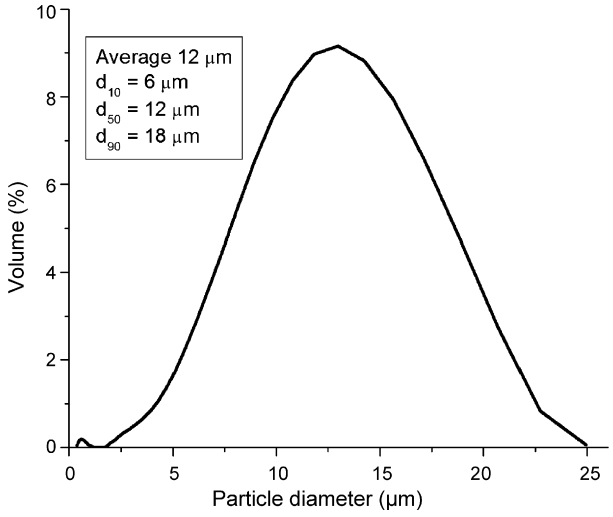

Fig. 2 – Size distribution of the spray-dried nanostructured titania agglomerates.

X-ray diffraction (XRD; Cu Kα radiation) was used to determine the phases present in the coatings and feedstock powder. A 2θ diffraction angle range from 20° to 60° (using a step size of 0.05° and step time of 2.5 s) was employed.

2.3. Microhardness and bond strength

Microhardness values of the coatings were measured using a Vickers microhardness tester with indentation loads of 300 gf for 15 s. A total of 10 microhardness measurements were performed for each coating. The ASTM standard C633-01 (ASTM, 2001) was followed to determine the degree of adhesion or bonding strength of the coatings to the substrates or the cohesive strength of the coating under tension normal to the surface. The loading rods were grit-blasted and attached to the surfaces of the coatings using a special adhesive-bonding tape (FM 1000, American Cyanamid, Wayne, NJ, USA). Five samples were tested for each spraying condition and the average value is reported.

3. Results and discussion

3.1. Nanostructured titania feedstock powder

A typical morphological structure of the agglomerated (spray-dried) and sintered nanostructure titania feedstock powder is shown in Fig. 1. It exhibits the typical donut-shape of spray-dried particles. When the powder is analyzed at high magnifications (Fig. 1b), it is possible to observe an agglomeration of titania nanoparticles smaller than 100 nm. Based on the results of Fig. 2, it is possible to observe that the majority of the spray-dried agglomerates exhibited diameters varying from 5 μm to 20 μm.

3.2. In-flight particle characteristics

In-flight particle diagnostics was performed in order to relate changes in the coating properties to changes in the in-flight particle temperature and velocity characteristics. Table 1 summarizes the average particle temperature and velocity for each spraying condition, whereas, Fig. 3 shows the particle temperature and velocity distributions in the thermal spray jet. The histograms show distributions that shift to higher particle temperature and velocity values as the propylene flow increases. The effect of propylene flow rate is significant and noteworthy. As the propylene flow increases, more particles exhibited temperatures at their surfaces above the melting point of titania (1855 °C (Miyayama et al., 1991)) and an increase in particle velocity was observed. During the HVOF spray processing, the powder particles are heated and accelerated at high speeds by the combustible gases. The maximum particle temperature and velocity values were obtained using the most fuel-rich conditions.

The dependence between particle temperature and velocity in the HVOF spraying of this powder is shown in Fig. 4. The correlation between particle temperature and velocity is

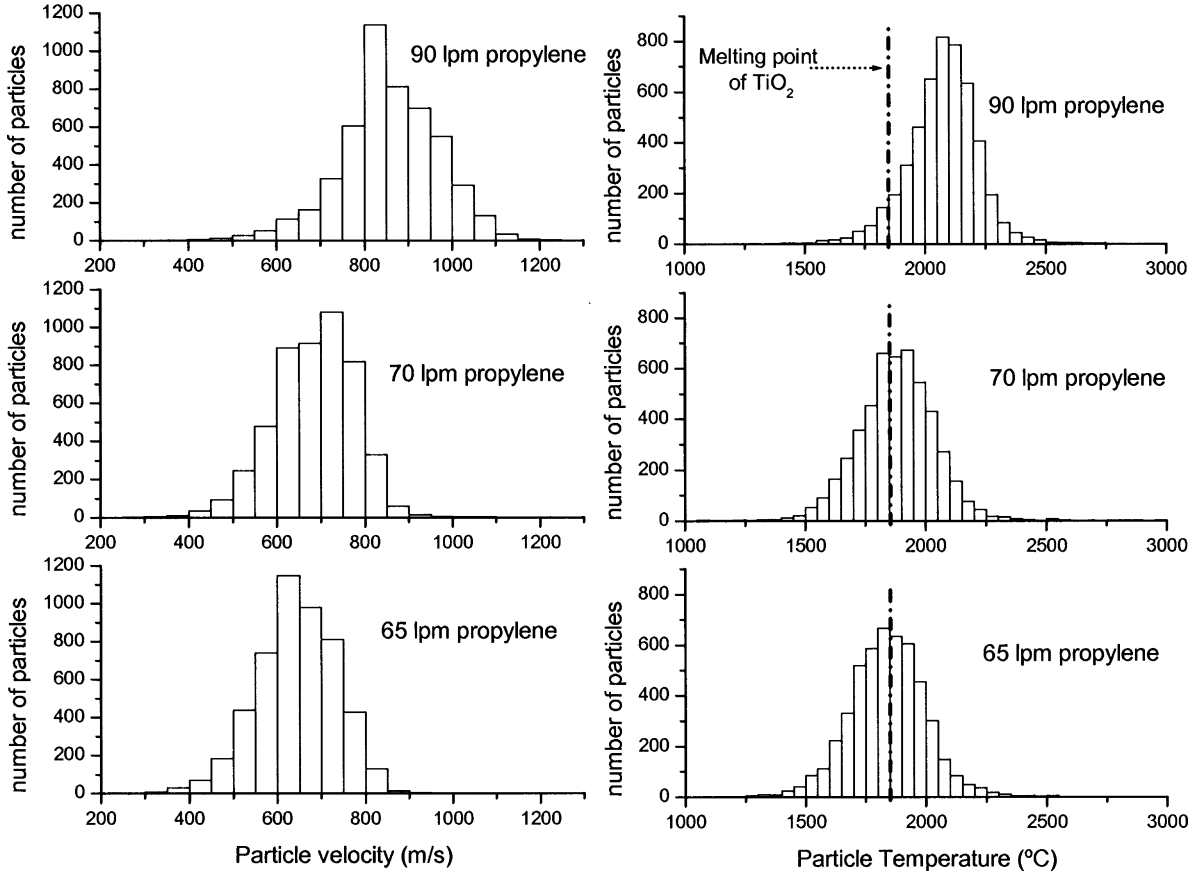

Fig. 3 – Histograms of the particle velocity and temperature ($n = 5000$).

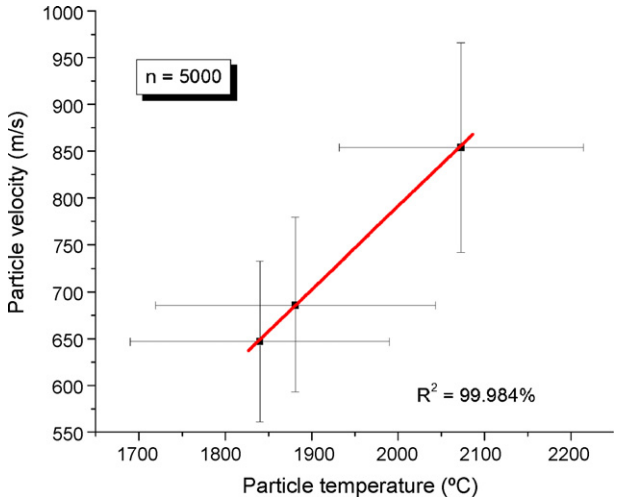

Fig. 4 – Dependence between particle temperature and particle velocity.

extremely important, because the majority of the microstructural characteristics of coatings will be derived from these two components. Higher particle temperatures will reduce the viscosity of the droplets, whereas, higher particle velocities will enhance the intersplat contact and reduce coating porosity, which will affect significantly the mechanical properties of the coatings. It is evident from this figure that from the range and conditions tested in this study, a linear dependence was established between average particle temperature and velocity. Such linear trend between particle temperature and velocity was also reported for the HVOF spraying of multimodal and conventional WC–Co powders, for different torches and spray parameters, using propylene, hydrogen and kerosene fuels (Marple and Lima, 2005). Therefore it appears that this is typical behaviour of HVOF processing, when the particle detector is placed at the same spray distance as used when depositing the coatings.

3.3. *Microstructural characterization*

The SEM images of the cross-section microstructures of the coatings can be observed in Fig. 5. Thermal spray coatings are known for their lamellar microstructure (Pawlowski, 1995), but in this case for the HVOF-sprayed nanostructured titania coatings, the traditional splat structure of the thermal sprayed coatings was not observed. When analyzing the cross-section of the HVOF-sprayed coating produced at 90 lpm of propylene, it can be observed that this coating exhibited an isotropic-like

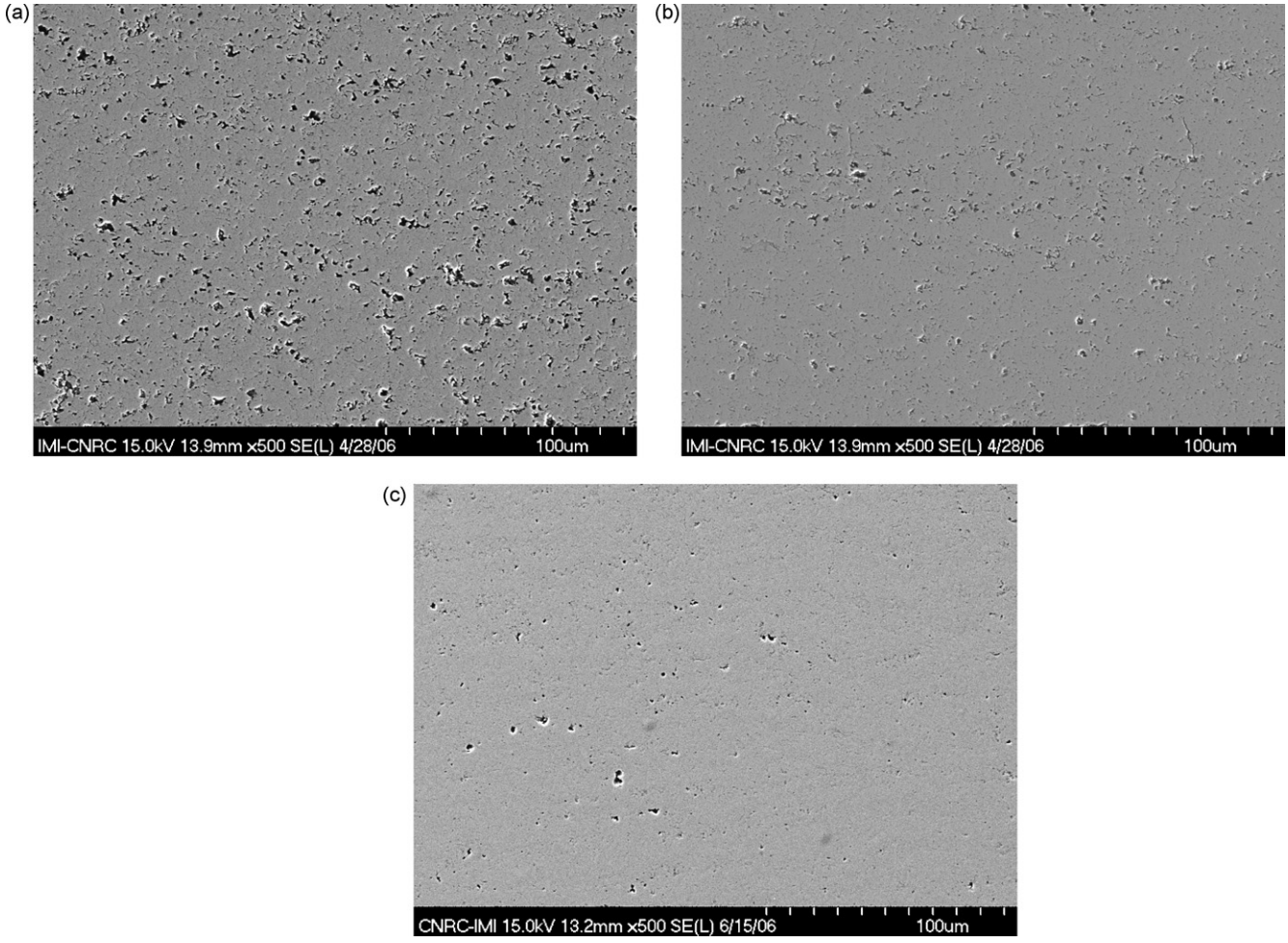

Fig. 5 – SEM cross-section images of the different coatings: (a) 65 lpm propylene, (b) 70 lpm propylene and (c) 90 lpm propylene.

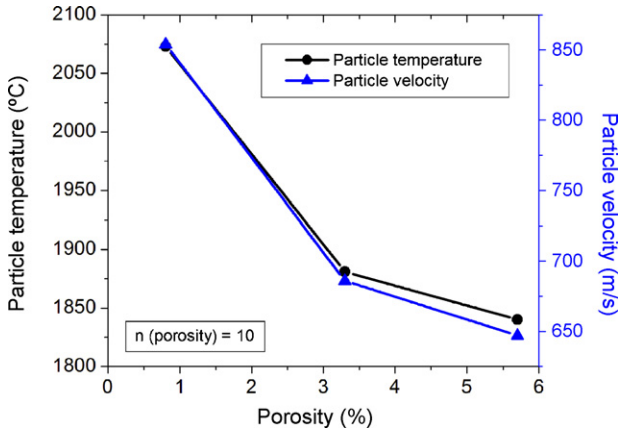

Fig. 6 – Combined effect of average particle temperature and velocity on the porosity levels of the HVOF-sprayed nanostructured titania coatings.

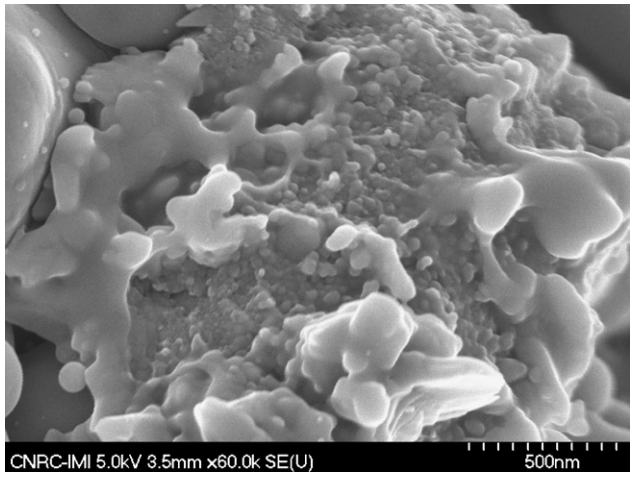

Fig. 7 – Nanotexture formed by a semi-molten agglomerate on the surface of an HVOF-sprayed nanostructured titania coating (Lima and Marple, 2007).

microstructure, with characteristics very similar to those of "bulk" materials.

The dependence involving average particle temperature and velocity with porosity can be observed in Fig. 6. It is generally accepted that higher values of particle temperature and velocity result in lower levels of porosity in coatings. For engineering coatings with given porosity levels, it is interesting to determine how these two factors would influence the porosity in these HVOF-sprayed ceramics, which was not known. Coating porosity decreases with increasing particle temperature and velocity values, which both affect the porosity levels. The measured porosity is below 1% for average particle temperature and velocity levels at $2073 \pm 141\,^{\circ}C$ and 854 ± 112 m/s, respectively. The porosity values obtained for the other two sets of spray parameters are similar to or lower than those for coatings produced via air plasma spray (APS), where particle temperatures are higher and particle velocities are lower than for HVOF. In the case of HVOF, the relatively high density of the nanostructured TiO_2 coatings is due the high-kinetic energy levels imparted to the sprayed particles. This favours particle/droplet deformation at impact and leads to better filling of the surface pores and irregularities (Ctibor et al., 2006; Du et al., 2005).

The dependence among porosity, particle temperature and particle velocity explored in this study are very pertinent. Engineering structures and coatings with different porosity levels can be very important in biomedical applications. For orthopaedic applications some authors (Eggli et al., 1998; Chang et al., 2000) have proposed porous structures and large interconnected pores that support cell attachment, which are progressively filled with mature new bone tissue. These porous structures would tend to provide enhanced osteointegration in implants. However, near pore-free coatings, such at that of Fig. 5c, may protect metallic prosthesis from environmental attack and reduce the possible release of ions from the underlying implant to body fluids and surrounding tissue (Okazaki et al., 2004). In addition, it has been reported that nanosized surface textures will exhibit an advantage in the interaction between the implant and bone cells. It was shown that the nanotopographies of different materials enhance the adsorption of ECM adhesion proteins that interact with osteoblast cells (Gutwein and Webster, 2004; Webster et al., 2000). An example of nanotexture on the surface of the HVOF-sprayed nanostructured titania coatings is shown in Fig. 7 (Lima and Marple, 2007). The structure is the result of a semi-molten particle (like that of Fig. 1) that was deposited on the surface of the coating.

3.4. *Residual stress*

Almen strips were used to compare the effect of the different particle temperature and velocity levels on the residual stresses. By looking at Fig. 8 it can be observed that there is a strong linear dependence between average particle characteristics (temperature and velocity) with the deflection of the Almen strip. It was hypothesized that there may a strong dependence among these variables because particle temperature and velocity exhibit major influences on the generation of residual stress. Despite this linear dependence, it is important

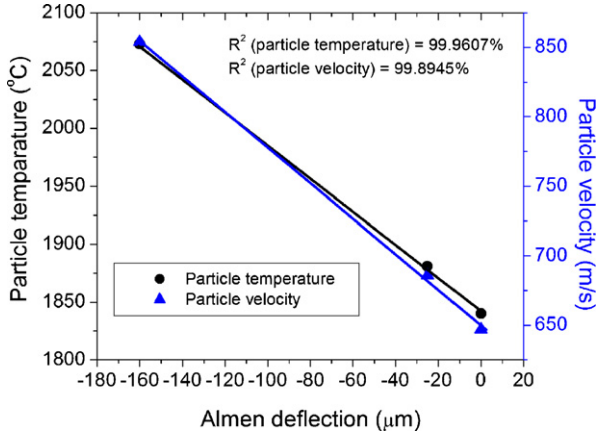

Fig. 8 – Combined effect of average particle temperature and velocity on the residual stress levels of the HVOF-sprayed nanostructured titania coatings.

to point out that Almen strips provide a qualitative indication of residual stress, therefore, there is not necessarily a linear dependence involving particle characteristics with residual stress levels. At the lowest particle temperature and velocity values, it was possible to produce a coating without significant levels of residual stress; however, for coatings produced under higher values of particle temperature and velocity, it was clearly observed that compressive residual stress levels were present, i.e., negative values of Almen strip deflection. Compressive residual stress plays an important role with respect to the operating performance of the coatings. It may restrain crack propagation throughout the coating and has a beneficial effect on the fatigue life (McGrann et al., 1998); however, excessive compressive stress levels may lower the bond strength of the coating.

These compressive residual stress levels produced during HVOF spraying are considered to be generated by different factors. One of the most important aspects is the high velocity of the impinging molten and semi-molten particles, creating a peening effect, generating compressive stresses that may extend into the substrate (Bansal et al., 2006). Therefore, the higher the particle velocity, the higher the compressive residual stress, as observed in Fig. 8.

Moreover, Stokes and Looney (Stokes and Looney, 2001) have indicated that during coating deposition when molten or semi-molten sprayed particles impinge on a surface, the particles shrink due to quenching and a compressive residual stress is created as the coating is built up. It can be hypothesized that when the particles are sprayed at higher velocities and temperatures the following effects occur: (i) the higher velocities would improve intersplat contact (reducing porosity, Figs. 5 and 6), enhancing heat transfer from the re-solidifying particle to the coating, (ii) this enhanced heat transfer would lead to higher localized temperatures and tend to maximize quenching effects, thereby also maximizing residual stress levels.

3.5. *Phase composition*

Fig. 9 shows the XRD patterns of the nanostructured feedstock and coatings. Only rutile and anatase phases were detected in

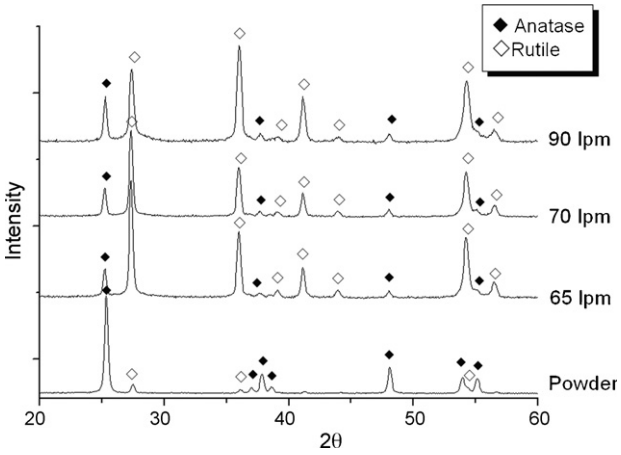

Fig. 9 – XRD patterns of the feedstock and the HVOF nanostructured titania coatings.

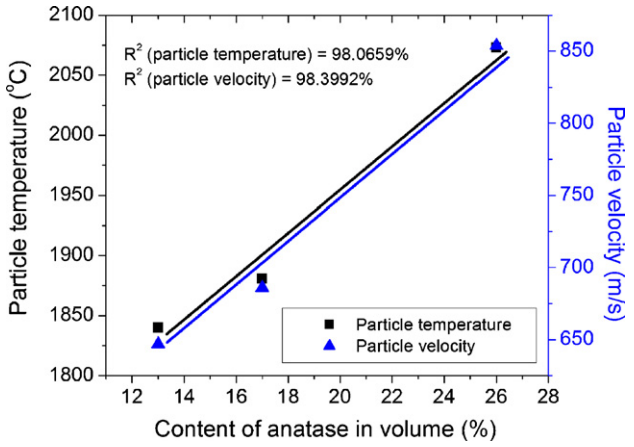

Fig. 10 – Combined effect of average particle temperature and velocity on the anatase content levels of the HVOF-sprayed nanostructured titania coatings.

all samples. Rutile is the stable phase of the three polymorphic forms of titania at atmospheric pressure, whereas anatase and brookite are metastable and transform irreversibly to rutile in the range of 400–1000 °C (Miyayama et al., 1991). The starting temperature and velocity of the anatase–rutile transformation is affected by factors such as impurities and particle size, among others (Miyayama et al., 1991).

Fig. 10 shows the effect of average particle temperature and velocity on the anatase content in the coatings. The volume percentage of anatase (C_A) was determined according to the following Eq. (1) (Berger-Keller et al., 2003):

$$C_A = \frac{8I_A}{13I_R + 8I_A} \times 100 \quad (1)$$

where I_A and I_R are the X-ray intensities of the anatase (1 0 1) and the rutile (1 1 0) peaks, respectively. Anatase was the predominant phase in the original feedstock. However, after HVOF spraying, the major phase was rutile and residual anatase represented a minor phase. By looking at Fig. 10 it is possible to observe a relatively strong linear dependence involving particle temperature and velocity with the content of anatase in the coatings. It is possible to observe that higher values of particle temperature and velocity induced higher contents of anatase (the major feedstock phase) in the coating microstructure.

The anatase phase found in these coatings was probably the result of semi-molten feedstock particles that became embedded in the coating microstructure after thermal spraying. An example of an embedded semi-molten particle is found in Fig. 11. It is important to point out that the temperatures of the particles measured in this study (via pyrometry) are surface temperatures. The maximum temperature of a propylene flame of the HVOF torch is below 3000 °C. These maximum temperature levels are much lower than those of plasma spray jets, which may reach 15,000 °C (Pfender, 1988).

By looking at Fig. 3, it can be observed that for a 90 lpm flow of propylene, the majority of the sprayed particles exhibited "surface" temperatures higher than that of the melting point of titania, which is 1855 °C (Miyayama et al., 1991). From the

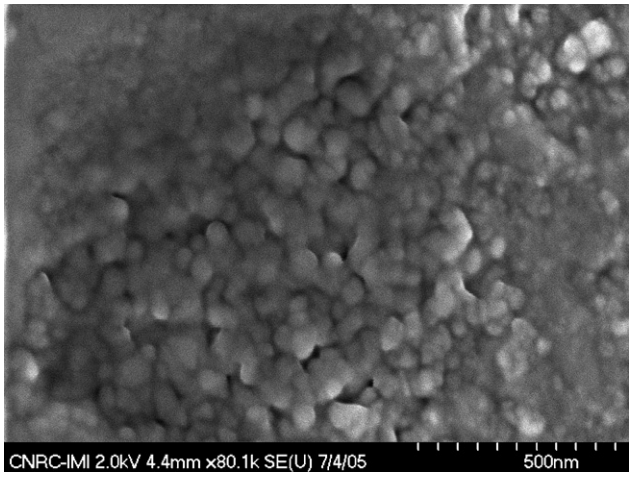

Fig. 11 – High magnification view of an HVOF-sprayed titania coating showing a semi-molten particle (as that of Fig. 1), embedded in the coating microstructure (Lima and Marple, 2007).

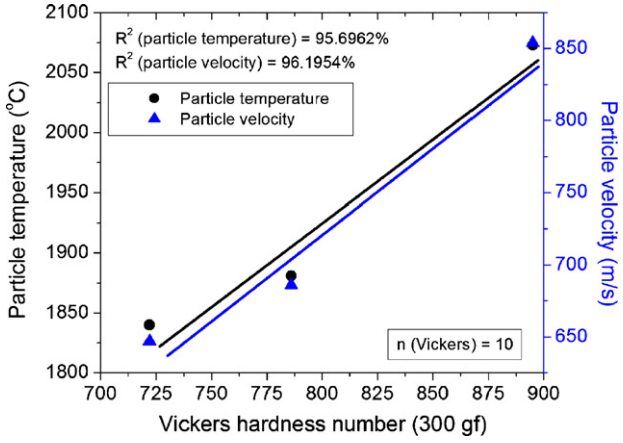

Fig. 12 – Combined effect of average particle temperature and velocity on the Vickers hardness numbers (300 gf) of the HVOF-sprayed nanostructured titania coatings.

results of Fig. 3, one can conclude that not only the smaller but also the larger particles from the powder distribution (Fig. 2) were successfully deposited on the substrate surface. Due to the relatively low temperatures of the HVOF flame (compared to those of APS), it is hypothesized that a fraction of the larger particles of the feedstock was not fully molten during the dwell time in the HVOF flame, i.e., the inner core of these particles exhibited temperatures below that of the melting point of titania. These non-molten cores (particles) deposited on the coating surface and became embedded in the coating microstructure (as shown in Figs. 7 and 11). It is this process that probably leads to higher contents of anatase phase for higher particle temperature and velocity values (Fig. 10). Due to these experimental observations, it was hypothesized that there was a dependence involving particle temperature and velocity, and content of anatase phase. This dependency is shown in Fig. 10. The deposition efficiency (DE) values agree with this hypothesis. The maximum DE values for propylene flows of 65 lpm, 70 lpm and 90 lpm (Table 1) were 36%, 46% and 54%, respectively.

It is important to highlight that higher amounts of anatase phase for APS titania coatings were observed when plasma spraying was carried out at lower power levels, employing plasma gas mixtures that resulted in lower thermal conductivities. Berger-Keller et al. (Berger-Keller et al., 2003) also attributed to semi-molten titania particles the higher anatase content of those coatings, however, some anatase phase may have formed from the melt upon resolidification. Finally, due to the high particle velocities and short spray distances employed in this work (Table 1), it is estimated that the non-molten cores would be subject to high temperatures for milliseconds, which would probably impede solid phase transformation from anatase to rutile.

3.6. *Hardness and bond strength*

The dependence involving Vickers microhardness numbers (300 gf) with average particle temperature and velocity can be seen in Fig. 12. As previously mentioned for other properties, particle temperature and velocity have a major role in the microstructure formation of coatings, which will affect the mechanical properties, such as hardness. It is possible to observe a relatively strong linear dependence involving particle temperature and velocity with the hardness values of the coatings. Higher particle temperatures and velocities enhance the intersplat contact, thereby increasing the cohesive strength of the coating. It is important to point out that hardness numbers varied from ~700 to ~900 (Fig. 12). These values are higher than those reported for bulk HA samples, which were sintered at temperatures in the range of 1250–1350 °C. In that study, the highest Vickers hardness number (300 gf) obtained was 513 ± 52 (Lopes et al., 1999). Therefore, these HVOF-sprayed nanostructured titania coatings exhibit cohesive strength levels higher than those of bulk HA.

All nanostructured titania coatings failed at the epoxy glue during bond strength testing (ASTM C633-01) (ASTM, 2001). Because these samples exhibited glue failure, the exact bond strength of these coatings could not be quantified. The strength of the epoxy glue was previously tested and indicated a value of 77 MPa (~11,000 psi), therefore, the bond strength values of all nanostructured titania coatings produced in this study were higher than this value. It was already observed that HVOF-sprayed nanostructured titania coatings exhibit high bond strength values when deposited on low carbon steel substrates (56 MPa to ~8000 psi) (Lima and Marple, 2006).

The higher bond strength of the nanostructured coatings was explained by a higher interfacial toughness observed by Bansal et al. for APS nanostructured ceramic coatings (Bansal et al., 2003). For conventional ceramic coatings it was observed that the interfaces between the particles that were fully molten in the spray jet and the steel substrate exhibited microcracks. For the nanostructured coating it was observed that the interfaces between the particles that were semi-molten in the thermal spray jet (i.e., dense nanozones-like that of Fig. 11) and the steel substrate were adherent, i.e., no microcracks or gaps. Therefore an interfacial crack in the nanostructured coating would tend to be interrupted by the strong adherent dense nanozones, thereby increasing

interfacial toughness and bond strength. In addition to this mechanism and the typical mechanical anchoring of the thermally sprayed splats on the grit-blasted substrate surface, a chemical reaction between the oxidized surfaces of the Ti-based substrate probably occurred with the titania particles, thereby enhancing the coating bond strength.

Although thermally sprayed HA coatings possess excellent biological and osteoconductive properties, the bond strength values of these coatings on Ti–6Al–4V substrates are lower than the values achieved for other bioceramic coatings. The bond strength of HVOF and APS hydroxyapatite coatings generally exhibits values below 31 MPa (Li et al., 2000). Therefore, the bond strength values of HVOF-sprayed coatings produced from nanostructured titania powders surpassed those of thermally sprayed HA coatings. This is a very important characteristic when selecting a biomedical coating.

It is important to point out that the previously unknown different dependencies obtained in this work, had the objective to predict or engineer the behaviour of these HVOF-sprayed nanostructured ceramic coatings. It is acknowledged that important fundamental science is behind all these dependencies, however, a fundamental understanding of these dependencies is beyond the scope of this work.

4. Conclusions

During this work, HVOF-sprayed nanostructured titania coatings were produced with different spraying conditions, in order to correlate particle temperature and velocity with the coating microstructure and properties, which will help to engineer future nanostructured and conventional ceramic coatings for different applications. The following conclusions were drawn:

- There is a linear dependence between particle temperature and particle velocity when spraying this type of powder using HVOF-spraying.
- There is a linear dependence involving average particle characteristics (temperature and velocity) and the deflection of Almen strips for these HVOF-sprayed coatings. The higher average particle temperatures and velocities induce higher compressive stress levels. These residual stress levels were probably caused by: (i) the impinging molten and semi-molten particles at the high-HVOF speeds, creating a peening effect and (ii) by the quenching and shrinking of molten and semi-molten sprayed particles on the surface, which generates compressive residual stress as the coating is built up.
- The major phase of the nanostructured feedstock powder is anatase, whereas the major phase of the HVOF-sprayed coatings is rutile. A relatively linear dependence involving the content of the anatase phase of the coatings with particle temperature and velocity. The higher the average particle temperature and velocity, the higher the content of the anatase phase. It is hypothesized that semi-molten feedstock particles embedded in the coating microstructure are responsible for the presence of the minor anatase phase in the coating.
- A relatively strong linear dependence involving particle temperature and velocity with the Vickers hardness numbers (300 gf) of the coatings was observed. The higher the average particle temperature and velocity, the higher the Vickers microhardness number. Higher particle temperatures and velocities enhance the intersplat contact, thereby increasing the cohesive strength of the coating. The Vickers hardness numbers (300 gf) obtained for the coatings were higher than that of the bulk HA.
- The bond strength values of all coatings were higher than 77 MPa (~11,000 psi) on Ti–6Al–4V substrates, which is higher than those reported for thermally sprayed HA coatings.
- It is hypothesised that the presence of semi-molten nanostructured particles in the coating surface (nanotexture) can have an important role in cell adhesion if these coatings are to be used in biomedical applications.

Acknowledgements

The authors thank J.-F. Alarie for metallography and adhesion testing, F. Belval for HVOF spraying, M. Lamontagne for in-flight particle diagnostics and M. Thibodeau for SEM observations. Moreover, M. Gaona thanks the Generalitat de Catalunya (Spain) for the Formació de Personal Investigador (FI) grant and the Thermal Spray Centre for the financial support.

REFERENCES

ASTM, 2001. Standard test method for adhesion or cohesion strength of thermal spray coatings. In: Annual Book of ASTM Standard C633-01. ASTM, West Conshohocken, PA, USA.

Bansal, P., Padture, N.P., Vasiliev, A., 2003. Improved interfacial mechanical properties of Al_2O_3-13 wt% TiO_2 plasma-sprayed coatings derived from nanocrystalline powders. Acta Mater. 51, 2959–2970.

Bansal, P., Shipway, P.H., Leen, S.B., 2006. Effect of particle impact on residual stress development in HVOF sprayed coatings. J. Therm. Spray Technol. 15 (4), 570–575.

Bauer, T.W., Geesink, R.C.T., Zimmerman, R., McMahon, J.T., 1991. Hydroxyapatite-coated femoral stems—histological analysis of components retrieved at autopsy. J. Bone Joint Surg. Am. 73A (10), 1439–1452.

Berger-Keller, N., Bertrand, G., Filiatre, C., Meunier, C., Coddet, C., 2003. Microstructure of plasma-sprayed titania coatings deposited from spray-dried powder. Surf. Coat Technol. 168, 281–290.

Castner, D.G., Ratner, B.D., 2002. Biomedical surface science: foundations to frontiers. Surf. Sci. 500 (1–3), 28–60.

Chang, B.S., Lee, C.K., Hong, K.S., Youn, H.J., Ryu, H.S., Chung, S.S., Park, K.W., 2000. Osteoconduction at porous hydroxyapatite with various pore configurations. Biomaterials 21 (12), 1291–1298.

Ctibor, P., Boháč, P., Stranyánek, M., Čtvrtlík, R., 2006. Structure and mechanical properties of plasma sprayed coatings of titania and alumina. J. Eur. Ceram. Soc. 26, 3509–3514.

Degasne, I., Baslé, M.F., Demais, V., Huré, G., Lesourd, M., Grolleau, B., Mercier, L., Chappard, D., 1999. Effects of roughness, fibronectin and vitronectin on attachment, spreading, and proliferation of human osteoblast-like cells (Saos-2) on titanium surfaces. Calcif. Tissue Int. 64, 499–507.

Du, H., Shin, J.H., Lee, S.W., 2005. Study on porosity of plasma-sprayed coatings by digital image analysis method. J. Therm. Spray Technol. 14 (4), 453–461.
Eggli, P.S., Muller, W., Schenk, R.K., 1998. Porous hydroxyapatite and tricalcium phosphate cylinders with two different pore size ranges implanted in the cancellous bone of rabbits. A comparative histomorphometric and histologic study of bony ingrowth and implant substitution. Clin. Orthop. Relat. Res. 232, 127–138.
Gutwein, L.G., Webster, T.J., 2004. Increased viable osteoblast density in the presence of nanophase compared to conventional alumina and titania particles. Biomaterials 25, 4175–4183.
Kasemo, B., 2002. Biological surface science. Surf. Sci. 500 (1–3), 656–677.
G.E. Kim, J. Walker Jr., J.B. Williams Jr., 2004, Nanostructured titania coated titanium, US Patent 6,835,449 B2, December 28.
Kim, G.E., 2006. Proven and promising applications of thermal sprayed nanostructured coatings. In: Marple, B.R., Hyland, M.M., Lau, Y.-C., Lima, R.S., Voyer, J. (Eds.), PDF file in Building on 100 Years of Success: Proceedings of the International Thermal Spray Conference 2006, May 15–18, 2006. Seattle, WA, USA. ASM International, Materials Park, OH, USA.
Legoux, J.G., Chellat, F., Lima, R.S., Marple, B.R., Bureau, M.N., Shen, H., Candeliere, G.A., 2006. Development of osteoblast colonies on new bioactive surfaces. J. Therm. Spray Technol. 15 (4), 628–633.
Li, H., Khor, K.A., Cheang, P., 2000. Effect of the powders' melting state on the properties of HVOF sprayed hydroxyapatite coatings. Mater. Sci. Eng. A 293, 71–80.
Lima, R.S., Marple, B.R., 2006. From APS to HVOF spraying of conventional and nanostructured titania feedstock powders: a study on the enhancement of the mechanical properties. Surf. Coat. Technol. 200, 3428–3437.
Lima, R.S., Marple, B.R., 2007. Thermal spray coatings engineered from nanostructured ceramic agglomerated powders for structural, thermal barrier and biomedical applications: a review. J. Therm. Spray Technol. 16 (1), 40–63.
Liu, X., Zhao, X., Fu, R.K.Y., Ho, J.P.Y., Ding, C., Chu, P.K., 2005. Plasma-treated nanostructured TiO_2 surface supporting biomimetic growth of apatite. Biomaterials 26, 6143–6150.
Lopes, M.A., Monteiro, F.J., Santos, J.D., 1999. Glass-reinforced composites: fracture toughness and hardness dependence on microstructural characteristics. Biomaterials 20, 2085–2090.
Marple, B.R., Lima, R.S., 2005. Process temperature/velocity-hardness-wear relationships for high-velocity oxyfuel sprayed nanostructured and conventional cermet coatings. J. Therm. Spray Technol. 14 (1), 67–76.
McGrann, R.T.R., Greving, D.J., Shadley, J.R., Rybicki, E.F., Bodger, B.E., Somerville, D.A., 1998. The effect of residual stress in HVOF tungsten carbide coatings on the fatigue life in bending of thermal spray coated aluminium. J. Therm. Spray Technol. 7 (4), 546–552.
Miyayama, M., Koumoto, K., Yanagida, H., 1991. Engineering properties of single oxides. In: Schneider, S.J. (Ed.), Engineered Materials Handbook, 4-Ceramic and Glasses. ASM International, Materials Park, OH, USA, pp. 748–757.
Okazaki, Y., Gotoh, E., Manabe, T., Kobayashi, K., 2004. Comparison of metal concentrations in rat tibia tissues with various metallic implants. Biomaterials 25, 5913–5920.
Pawlowski, L., 1995. The Science and Engineering of Thermal Spray Coatings. Wiley, West Sussex, England.
Petit, V., Thiery, J.P., 2000. Focal adhesions: structure and dynamics. Biol. Cell 92 (7), 477–494.
Pfender, E., 1988. Fundamental studies associated with the plasma spray process. Surf. Coat. Technol. 34, 1–14.
Sauer, J.P., Sahoo, P., 2001. HVOF process control using Almen and temperature measurement. In: Berndt, C.C., Khor, K.A., Lugscheider, E. (Eds.), Thermal Spray 2001: New Surfaces for a New Millennium. ASM International, Materials Park, OH, USA, pp. 791–796.
Stokes, J., Looney, L., 2001. HVOF system definition to maximise the thickness of formed components. Surf. Coat. Technol. 148 (1), 18–24.
Tjong, S.C., Chen, H., 2004. Nanocrystalline materials and coatings. Mater. Sci. Eng. R. 45, 1–88.
Wakai, F., Kondo, N., Shinoda, Y., 1999. Ceramics superplasticity. Curr. Opin. Solid State Mater. Sci. 4, 461–465.
Webster, T.J., Siegel, R.W., Bizios, R., 1999. Osteoblast adhesion on nanophase ceramics. Biomaterials 20, 1221–1227.
Webster, T.J., Ergun, C., Doremus, R.H., Siegel, R.W., Bizios, R., 2000. Enhanced functions of osteoblasts on nanophase ceramics. Biomaterials 21 (17), 1803–1810.
Zhao, X., Liu, X., Ding, C., Chu, P.K., 2006. In vitro bioactivity of plasma-sprayed TiO_2 coatings after sodium hydroxide treatment. Surf. Coat. Technol. 200, 5487–5492.